Effect of Cold Flakes on Mechanical Properties of Aluminum Alloy Die-Casts

A.K.M. Aziz Ahamed and Hiroshi Kato*

Graduate School of Science and Engineering, Saitama University, 255 Shimo-Okubo, Sakura, Saitama, Japan

The cold flake was detected in aluminum alloy die-casts ADC12 by using the scanning acoustic microscope (SAM), and was visualized in the acoustic image as bright and dark regions, which were corresponding to the oxide layer and the body of the cold flake, respectively. By using the specimen containing the cold flake, the tensile testing and the fatigue testing were carried out. The in-process ultrasonic measurement was also carried out with a water bag in the fatigue testing to detect detachment of the cold flake from the matrix in the fatigue process. From these results, it was found that the cold flake was detached from the matrix in the fatigue process to form a crack, and cold flakes, especially exposed cold flakes, reduce the tensile strength and the fatigue life of die-casts. The effect of the cold flake on the strengths was discussed from the point of crack propagation.

Keywords: Aluminum alloy die-casts, Cold flake, Ultrasonic measurement, Tensile strength, Fatigue strength

INTRODUCTION

Automobile parts are often produced by aluminum alloy die-castings and suffer repeated loading. In this regard, casting defects largely influence mechanical properties of die-cast products [1-6]. Among casting defects, interests have been concentrated in harmfulness of the cold flake, one of irregular structures [7-9]. The cold flake is formed when the molten metal is poured in a shot sleeve and pushed by a plunger, during which the initially solidified layer of the melt is broken into small parts in the castings. These small broken parts inside the castings are called cold flakes, and are generally covered by oxide layer contaminated with lubricants and accompanied by pores [10] to reduce wettability with the matrix. Hence, mechanical properties and reliability of aluminum alloy die-casts are decreased with the amount of the cold flake [11]. With the current production technology, the defects are unavoidable [12], and hence it is required to verify their influence on mechanical properties quantitatively.

The aim of the present study is to examine the effect of the cold flake on the tensile strength and the fatigue life of the aluminum alloy die-casts ADC12.

Corresponding author: hkato@mech.saitama-u.ac.jp

EXPERIMENTAL PROCEDURE
Specimen Preparation
In the present work, aluminum alloy die-cast plates (ADC12, nominal composition of Al - 11 mass% Si - 2.5 mass% Cu) with a thickness of 4 mm were produced by using wider gates and longer shot time lags in the injection process, to include greater cold flakes in the die-cast plates. The scanning acoustic microscopy was carried out with a probe generating a longitudinal wave of 50 MHz in frequency and with a focal distance of 12 mm in water to obtain acoustic images at positions 2 mm below the surface. The acoustic image of 72 mm $\times$ 234 mm in area was composed of 52 segments with an area of 18 mm $\times$ 18 mm. **Figure 1** shows a part of an acoustic image. In the figure, the bright and dark segments are the oxide layer and the body of the cold flake, respectively. By selecting the cold flake in the plate, rectangular pieces were cut from the plate. And then, as shown in **Figs. 2 and 3,** specimens for tensile testing and fatigue testing were prepared, respectively, with the cold flake of different sizes at a required position.
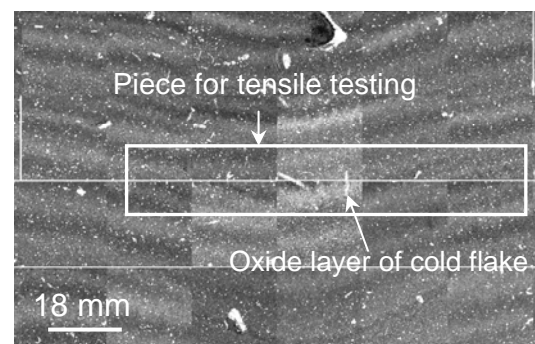

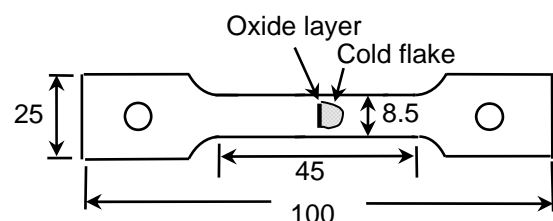Fig. 1   Acoustic image of die-cast plate.

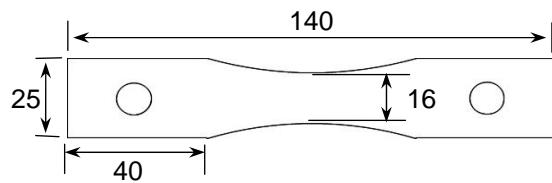Fig. 2   Shape of specimen for tensile testing.

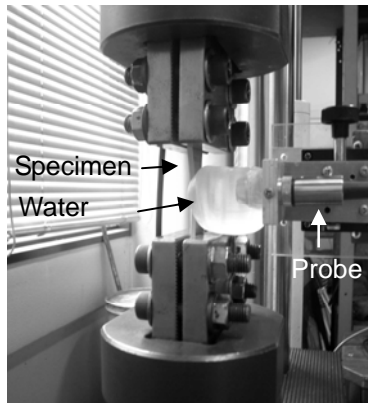Fig. 3 Shape of specimen for fatigue testing.

Fig. 4 Setup for in-process ultrasonic measurement during fatigue testing.

Mechanical Testing

The tensile testing was carried out to fracture with a crosshead speed of 0.5 mm/min to obtain the effect of the cold flake on the tensile strength.

The fatigue testing was performed at a stress ratio of R= 0.05 (tension-tension type) and a frequency of 10 MHz. Specimens that did not fail at one million cycles or more were considered run-out. First, the fatigue testing was carried out with different stress amplitudes to obtain an S-N diagram. Then the fatigue testing was conducted under a stress amplitude of 65 MPa to examine the effect of the cold flake on the fatigue life (the number of cycles to failure).

After mechanical testings, fracture surfaces were observed through optical microscope and scanning electron microscope (SEM) in order to specify a site of crack initiation.

In-Process Ultrasonic Measurement

At required numbers of fatigue cycles, the fatigue tester was paused and held at a mean load of the fatigue cycle. Then the in-process ultrasonic measurement was carried out with a water bag to examine detachment of the cold flake from the matrix during fatigue testing, with a probe of 20 MHz in frequency and a focal distance of 25.4 mm in water, as shown in **Fig. 4**. In the measurement, the ultrasonic wave was focused on the cold flake inside the specimen.

RESULTS AND DISCUSSION
Effect of Cold Flake on Tensile Strength

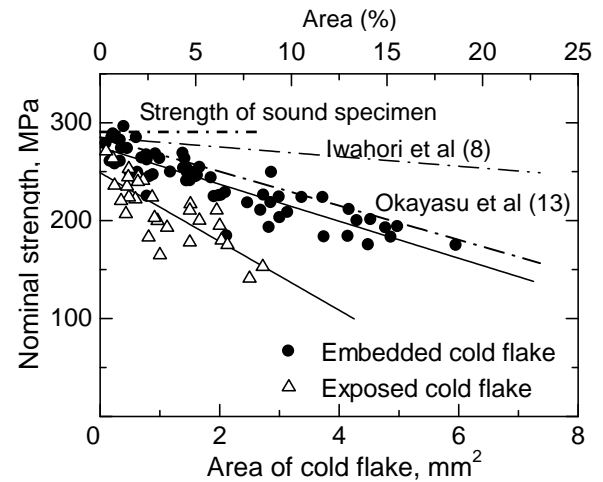**Figure 5** shows a relation between the nominal tensile

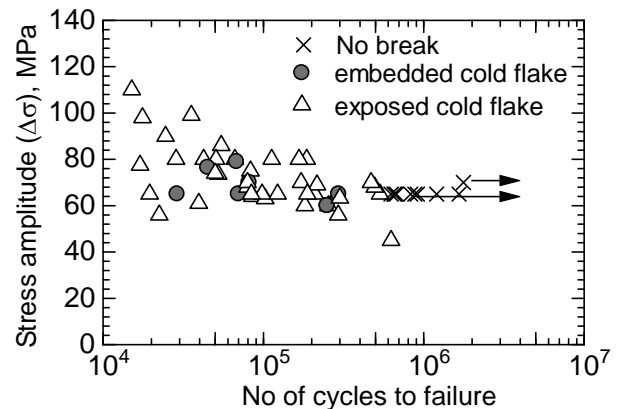Fig. 5 Change in nominal tensile strength with area of oxide layer of cold flake.

Fig. 6 S-N curve for the alloy ADC12.

strength and the area of the oxide layer of the cold flake (hereafter referred to as the area of the cold flake). In the figure, regression solid lines were drawn for embedded and exposed oxide layers of the cold flake using the least square fitting. The dotted line shows the tensile strength (about 285 MPa) of the sound specimen without coarse cold flakes. The area of the cold flake has a deleterious effect on the tensile strength, and moreover when the cold flake was exposed to the surface, the tensile strength was largely reduced. Iwahori et al. [8] and Okayasu et al. [13] measured the tensile strength of aluminum alloy die-casts ADC12 and ADC10 containing cold flakes, and found decreasing tendency of the tensile strength with the amount of the cold flake as compared in **Fig. 5**. The difference in the tensile strength between the present study and results of Iwahori et al. and Okayasu et al. is explained by difference in estimation of the area of the cold flake on the fracture surface.

Effect of Cold Flake on Fatigue Life

Results of the fatigue testing are shown in **Fig. 6**, where the fatigue life is plotted against the nominal stress amplitude. The fatigue life largely scatters in all stress
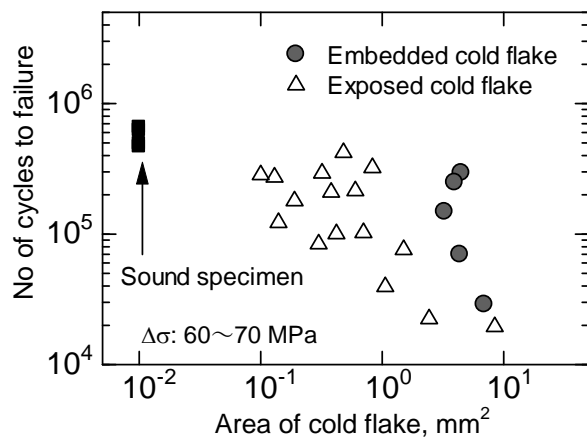
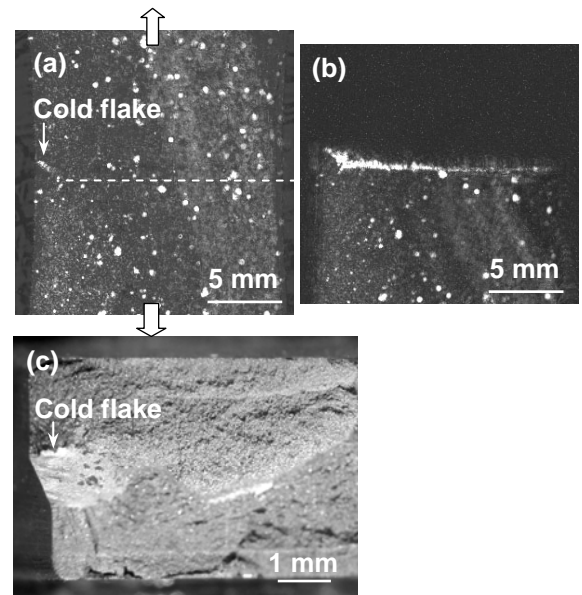Fig. 7 Effect of area of cold flake on fatigue life.

Fig. 8 Comparison of acoustic image and fracture surface of specimen containing small exposed cold flake. (a) acoustic image before testing, (b) acoustic image after fracture and (c) fracture surface.
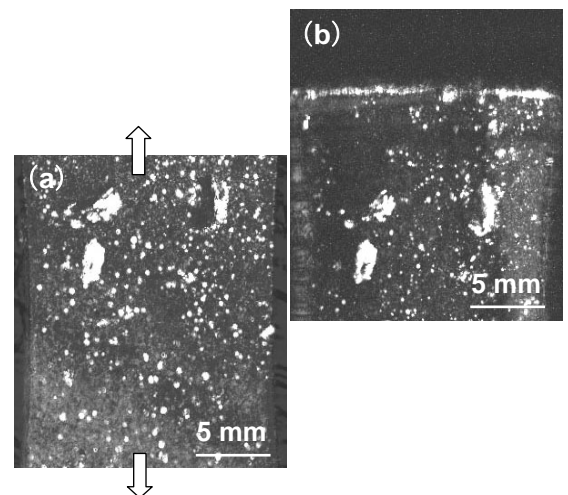
amplitudes. From observation of the fracture surface, the crack initiated not only from the embedded cold flake but also from the exposed cold flake, which caused the scatter of the fatigue life as well as the size of the cold flake.

Figure 7 shows the effect of the area of the cold flake on the fatigue life at a stress amplitude of 60～70 MPa. In the figure, the sound specimen was considered as a specimen with a crack initiation site of 200 μm or less in size. With increasing area of the cold flake, the fatigue life largely decreased, and the exposed cold flake is more severe for the fatigue life than the embedded one.

Fracture Behavior

A relation between the crack propagation and the arrangement of the cold flake was examined. **Figure 8** compares acoustic images before and after fatigue testing and a fracture surface of the specimen with a small cold flake exposed to the side surface. In the figure, the loading direction was vertical, and a dotted line shows a crack propagation path from the cold flake, and it was confirmed by the fracture surface, as shown in **Fig. 8 (c)**. **Figure 9** shows a case of an embedded large cold flake directing parallel to the loading direction. In this case, the fracture occurred at a different position from the observed cold flake, and an exposed cold flake perpendicular to the loading direction acted as a crack initiation site.

Further examination was carried out in order to determine the initiation point for cold flakes of different sizes. **Figure 10** shows a crack initiation site with a size of about 200 μm or less observed in the sound specimen.

Figure 11 shows crack initiation and propagation from a small cold flake of about 400 μm in size. From the fracture surface, it was confirmed that the unstable fracture occurred after fatigue crack propagation.

Figure 12 shows the case that the fracture occurred from an embedded large cold flake. In the figure, there are three distinguished regions, the oxide layer of the cold flake, the region of the fatigue crack propagation, and the region of the unstable crack propagation.

Fig. 9 Comparison of acoustic images (a) before testing and (b) after fracture.

Figure 13 shows enlarged views of three different regions. The first photograph (a) shows the oxide layer of the embedded cold flake (the region I), the second one (b) shows the region of the fatigue crack propagation (the region II), and the third one (c) shows the region of the unstable fracture (the region III). The region II is generally characterized by striations, but in the present work, no striations were observed on the fracture surface. However, the region II was clearly distinguished from the region III containing dimples.

Cold flakes were identified as the initiation site of the fatigue crack in all specimens except the case of sound specimens. The reason why the cold flake acts as a preferred crack-initiation site is explained as follows. The Young's modulus of the aluminum oxide (Al_2O_3)
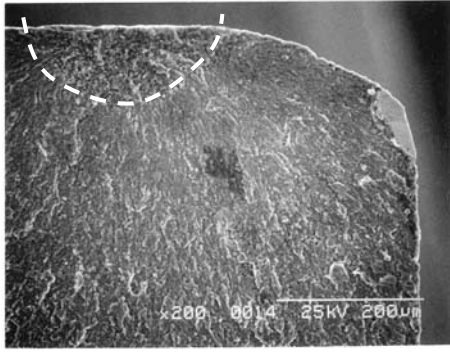
Fig. 10   Fracture surface of sound specimen in which crack initiated at side surface.
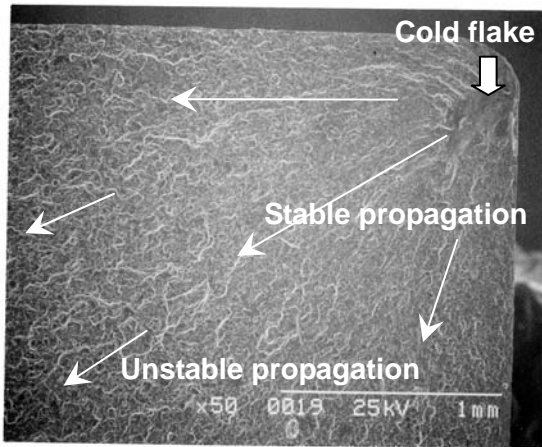

Fig. 11   Fracture surface showing crack propagation from small exposed cold flake.
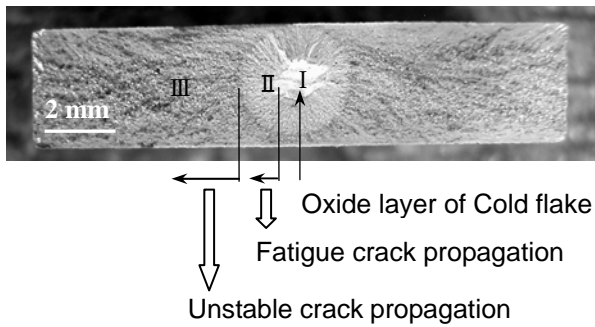

Fig. 12   Fracture surface showing crack propagation from large embedded cold flake.
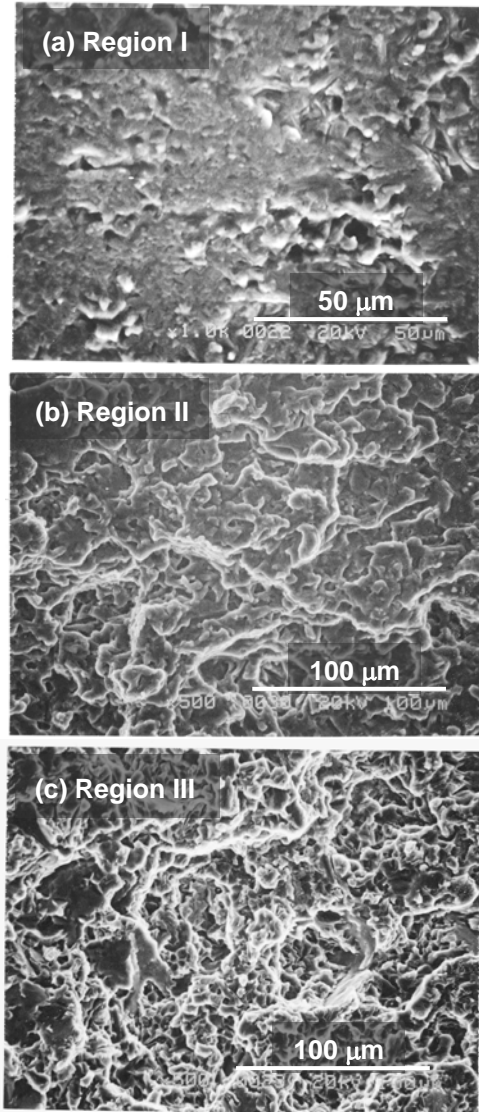

Fig. 13   Enlarged views of three regions in fracture surface: (a) oxide layer of cold flake, (b) region of fatigue crack propagation, (c) region of unstable crack propagation.

formed on the surface of the cold flake is about 300 GPa, and is significantly greater than that of the matrix of 70 GPa.   Therefore, a high stress concentration is generated around the oxide layer to cause accumulation of fatigue damaging to result in initiation of a fatigue crack.

Change in Ultrasonic Wave in Fatigue Process
In the previous works [14, 15], the authors carried out the ultrasonic measurement of the specimen containing the cold flake, and showed that the cold flake stuck to the matrix before tensile testing, and was detached from the

matrix before final failure in the tensile testing.   Hence, the in-process ultrasonic measurement was carried out in the fatigue testing to examine detachment of the cold flake from the matrix.   **Figure 14** shows the measured cold flake embedded in the specimen.   During fatigue testing, echoes reflected from the surface and the bottom of the specimen and the cold flake were observed as shown in **Fig. 15**.

At an early stage of the fatigue process, as shown in Fig. 15 (a), the surface echo pointed downward and the bottom echo pointed upward.   And, the echo reflected from the cold flake (R_{CF}) pointed downward as the surface echo.

At a later stage of the fatigue process, the direction of the echo R_{CF} changed from downward to upward as shown in Fig. 15 (b).   The change in the direction of the echo is due to the change in the reflection condition at the boundary between the cold flake and the matrix.
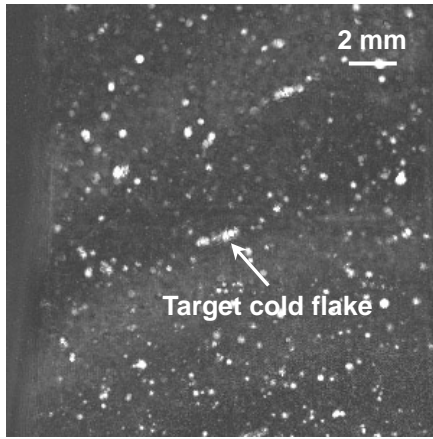
Fig. 14 Acoustic image of target cold flake for in-process measurement.

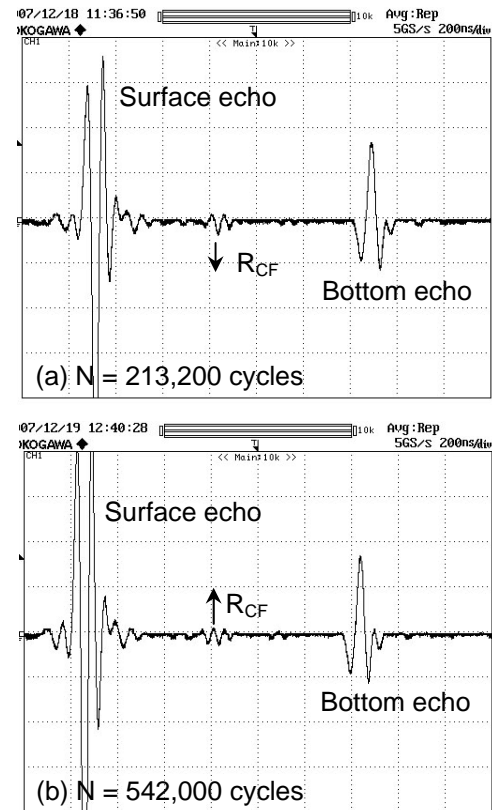(a) N = 213,200 cycles

(b) N = 542,000 cycles

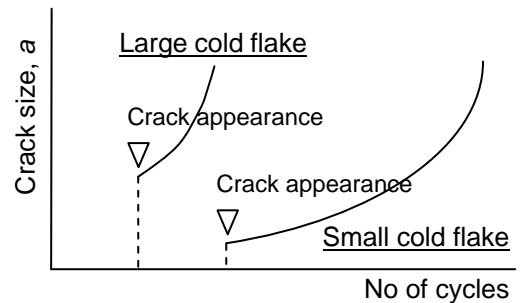Fig. 15 Change in ultrasonic wave reflected from cold flake during fatigue testing.

Fig. 16 Change in crack size after appearance with number of fatigue cycles for cold flakes of different sizes.

When the cold flake stuck to the matrix, the ultrasonic wave was reflected from the oxide layer, and the reflection echo shows the same direction as the surface echo, but when the cold flake was detached from the matrix, the ultrasonic wave was reflected from the space between the cold flake and the matrix, and the reflection echo shows the opposite direction from the surface echo. Therefore, from the change in the direction of the echo reflected from the cold flake, it was found that the cold flake was detached from the matrix to form a crack. The specimen broke at 641,500 cycles, but unfortunately, the fracture occurred at another cold flake, and it was unable to observe the crack propagation from the observed cold flake.

Evaluation of Maximum Stress Intensity Factor at Failure

Figure 16 shows a schematic representation of crack appearance and propagation.

In the case of the large cold flake, the cold flake detaches from the matrix at a smaller number of cycles to a critical size being determined by the critical stress intensity factor amplitude ΔK_{IC}. In this case, the fatigue life is relatively shorter.

In the case of the small cold flake, the cold flake detaches from the matrix at a larger number of cycles, and then propagates to the critical size ΔK_{IC}, and the fatigue life is relatively longer.

The final failure occurs when the stress intensity factor amplitude reaches the critical value ΔK_{IC}, as represented schematically in Fig. 17. And, when the stress amplitude is fixed, the final size of the crack determines the critical value ΔK_{IC} independently on the size of the cold flake. In other words, the critical value ΔK_{IC} is obtained by the crack size at final failure.

In the case of the embedded cold flake, the region of the fatigue crack propagation was clearly identified as shown in Fig. 12. Therefore, assuming that the unstable crack propagation occurred when the crack size reached the critical size, the maximum value of the stress intensity factor amplitude (K_{Imax}) was calculated by using stress intensity factors obtained by Murakami [16], and also by Ishida and Noguchi [17]. The final shape of the crack was considered as a circle as shown in Fig. 12. In **Fig. 18**, the maximum stress intensity factor K_{Imax} obtained by two equations are plotted in a range of 8 ~ 11 MPa.m$^{1/2}$. This value was coincident with the critical stress intensity factor $K_{Icritical}$ at failure of 8 ~ 10 MPa.m$^{1/2}$ obtained in the tensile testing [14, 15].
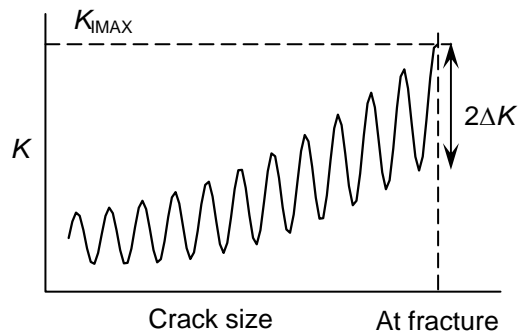
CONCLUSIONS

Fig. 17 Change in stress intensity factor with crack size in fatigue process.
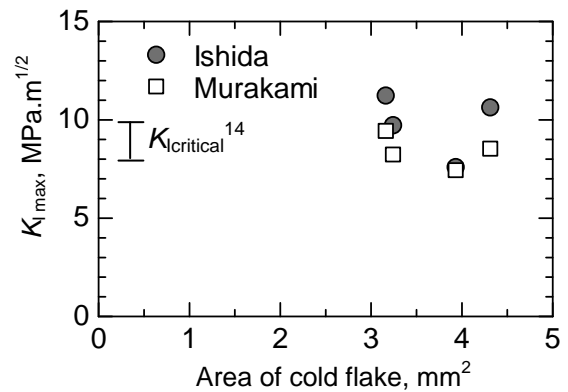

Fig. 18 Maximum stress intensity factor for embedded cold flake determined from area of crack at final fracture.

The tensile and the fatigue testings were conducted with the aluminum alloy die-cast plate (ADC12) containing the cold flake. And, the in-process ultrasonic measurement was also carried out in the fatigue testing. Then following conclusions are drawn.

(1) The tensile strength decreased with the size of the cold flake. Especially the exposed cold flake reduced the strength more greatly than the embedded one.

(2) The S-N relation was obtained by the fatigue testing but showed a large scatter, because of difference in size and position of the cold flake. The fatigue life was largely reduced with the area of the cold flake. The exposed cold flake perpendicular to the loading direction reduced the fatigue life far greatly than the embedded one.

(3) The in-process ultrasonic measurement showed that the cold flake was detached from the matrix in the fatigue process to form a crack.

(4) The maximum stress intensity factor (K_{Imax}) was evaluated from the final crack size, and showed a valued of 8 ~ 11 MPa.m$^{1/2}$ for embedded cold flake, and was in good agreement with the critical stress intensity factor at failure obtained in the tensile testing.

REFERENCES

1. H. Mayer, M. Papakyriacou, B. Zettl and S.E. Stanzl-Tschegg: *Int. J. Fatigue*, 2003, **25**, 245-256.
2. J.Z. Yi, Y.X. Gao, P.D. Lee, H.M. Flower and T.C. Lindley: *Met Mate. Trans. A*, 2003, **34A**, 1879-1890.
3. J. Linder, M. Axelsson and H. Nilsson: *Int. J. Fatigue*, 2006, **28**, 1752-1758.
4. J. Linder, A. Arvidsson and J. Kron: *Fatigue and Fract. Eng. Mater. Struct.*, 2006, **29**, 357-363.
5. K. Kanazawa, M. Tachikawa, K. Shibayama and M. Shimamura: Trans. 1996 Japan Die Cast. Cong., Yokohama, Dec. 1996, Japan Die Casting Association, 129-135. (In Japanese)
6. S. Echigo, K. Kanazawa, K. Konagaya, S. Aoyama, H. Hirokawa and S. Watanabe: Trans 2002 Japan Die Cast. Cong., Dec. 2002, Japan Die Casting Association, 157-162. (In Japanese)
7. T Komazaki, Y Maruyama and N Nishi: *IMONO* 1995; **67**, 258-264. (in Japanese)
8. H. Iwahori, K. Tozawa, Y. Yamamoto and M. Nakamura: *J. Japan Inst. Light Met.*, 1984, **34**, 389-394. (in Japanese)
9. H. Nomura, E. Kato, Y. Maeda and S. Okubo: *J. JFS*, 2001, **73**, 656-661. (in Japanese)
10. C. H. Caceres and B. I. Selling: *Mater. Sci. and Eng. A*, 1996, **220**, 109-116.
11. R. Kimura, M. Yoshida, G. Sasaki and J Pan and H. Fukunaga: *J. Mater. Process Technol.*, 2002, **130-131**, 299-303.
12. W.G. Walkington: 'Causes and solutions die-casting defects', 155-158; 1997, Rosemont, North American Die-casting Association Publication.
13. M. Okayasu, K. Kanazawa and N. Nishi: *J. JFS*, 1998, **70**, 779-785. (in Japanese)
14. A.K.M.A. Ahamed and H. Kato, *J. JFS*, 2007, **79**, 374-379. (in Japane*se)*
15. A.K.M.A. Ahamed and H. Kato: *Mater. Trans.* 2008, **49**. (in print)
16. Y. Murakami and H. Usuki: *Trans. Japan Mech. Eng. Soc.*, 1989, **55**, 213-221. (in Japanese)
17. M. Ishida and H. Noguchi: *Eng. Frac. Mech.*, 1984, **20**, 387-408.